P7.19

A Comparison of High Spectral Resolution Infrared Cloud Top Pressure Algorithms using S-HIS Measurements

Robert E. Holz, Paolo Antonelli, Steve Ackerman and Fred Nagel
University of Wisconsin CIMSS
Matthew McGill
Goddard Space Flight Center

Introduction

Cloud top pressure is an important parameter in determining the radiative impact of clouds on climate. In addition, atmospheric temperature and moister retrievals of cloudy scenes require that the cloud altitude be known. This paper presents a comparison of hyperspectral cloud top altitude retrievals using S-HIS data from THORPEX and TX2002 field experiments. Included in this comparison is CO_2 Sorting, a new hyperspectral cloud top retrieval algorithm designed to determine the optimal channel pairs to be applied to CO_2 Slicing. To investigate the performance of the hyperspectral cloud top retrievals collocated Cloud Physics Lidar (CPL) and Modis Airborne Simulator (MAS) measurements are compared.

Instrumentation

Scanning High-resolution Interferometer Sounder (S-HIS)

The Scanning High-resolution Interferometer Sounder (SHIS) is an aircraft based scanning Fourier transform interferometer designed to measure atmospheric infrared radiances at high spectral and spatial resolutions (Revercomb, H. E. et al., 1998). The S-HIS measures the infrared emission between 3.0 – 16 μm with a spectral resolution of approximately 0.5 wavenumbers. The radiometric calibration allows for RMS noise errors to less than 0.2 K in terms of brightness temperature across the spectral bands except for near the band edges where the calibration is degraded (Revercomb, H. E. et al., 1998). The S-HIS has a 100 mrad field of view and is capable of cross scanning. For the preceding analysis only nadir fields of view are used. With a flight altitude of 20 km the nadir S-HIS fields of view have a 2 km diameter surface footprint. The footprint is slightly oval along the flight track due to the 1-second dwell time and 200 m/s along track velocity.

Cloud Physics Lidar (CPL)

The Cloud Physics Lidar (CPL) is a cloud lidar developed by NASA Goddard and flies on the ER2 high altitude aircraft (McGill, M. et al., 2002). The CPL is an active remote sensing system, capable of very high vertical resolution cloud height determinations (30 meters), cloud visible optical depth, and backscatter depolarization. The depolarization measurement allows for the discrimination between ice and water clouds. Photons backscattered on the surface of spherical water droplets have very little depolarization in contrast to ice crystals where the backscatter results in large depolarization. For CPL measurements, depolarization of greater then 25% are ice while polarizations less then 10% are generally water clouds.

The CPL laser transmits at 355, 532, and 1064 nm and fires 5000 shots/sec. For this paper the 532 nm one second averaged data is used. The high sample rate of the CPL results in a surface footprint that can be approximated as a continuous line with a diameter of 2 meters. A robust collocation algorithm is used to collocate the CPL measurements with the S-HIS. On average, ten CPL are measurements are found in each 2-km S-HIS field of view. The collocated CPL measurements of cloud height, depolarization, and optical thickness are used in this paper to analyze the sensitivity of S-HIS cloud top retrievals.

MODIS Airborne Simulator (MAS)

The MODIS Airborne Simulator (MAS) is a scanning spectrometer with a 2.5 mrad field of view. The MAS scene mirror scans at 7.25/sec with a swath width of 42.96° from nadir resulting in a 50-meter nadir surface resolution with a swath width of 37.2 km at the 20 km ER2 flight altitude (King, M. D. et al., 1996). The MAS has 50 spectral channels located within the 0.55 – 14.2 μm spectral region. For this investigation the MAS high spatial resolution is utilized to provide information about the cloud fractional coverage in individual S-HIS field of view. To accurately determine the corresponding MAS pixels in the SHIS footprint, MAS is collocated with the SHIS using the collocation algorithm described in the Collocation of imager and sounder data section. The results of the collocation are applied to the MAS cloud mask (Ackerman et al 1998) and the cloud fraction of the S-HIS field of view is calculated. In this analysis if the MAS cloud mask determines the pixel to be cloudy or probably cloudy the pixel is designated cloudy. All other classifications are considered clear.

Algorithms and Methods

CO2 Slicing

The CO_2 Slicing algorithm has successfully retrieved cloud top pressure using broadband satellite measurements for over three decades. The method was developed to overcome errors in the height retrievals of partially cloudy fields of view and optically thin clouds (Smith, W. L., 1970: Smith, W. L. et al., 1978) (Menzel, W. P. et al., 1983). The method relies on the strong temperature sensitivity of the 15 µm CO_2 band and the well-mixed nature of carbon dioxide. More recently, CO_2 Slicing has been applied to hyperspectral aircraft measurements (Smith, W. L. et al., 1990). The CO_2 Slicing equation is as follows:

Equation 1

$$\frac{I(v_1)-I_{cl}(v_1)}{I(v_2)-I_{cl}(v_2)}=\frac{\varepsilon_1\int_{ps}^{Pc}\tau(v_1,p)\frac{dB\left[v_1,T(p)\right]}{dp}dp}{\varepsilon_2\int_{ps}^{Pc}\tau(v_2,p)\frac{dB\left[v_1,T(p)\right]}{dp}dp}$$

Where *I* is the measured radiance in channel v_1, the subscripts reference the two channels selected for the retrieval. I_{cl} is the clear sky radiance, ε is the cloud fractional emissivity, $\tau(v_1,p)$ is the channel transmittance between the pressure levels p to the instrument, and $B\left[v_1,T(p)\right]$ is the Plank radiance for the selected channel frequency at pressure level *p*. In the current application, both $I\ (v_{cl})$ and $\tau(v,p)$ are computed using temperature and moisture profiles retrieved from clear sky SHIS measurements. The clear sky radiance and transmittance are computed using a line-by-line clear-sky radiative transfer model (LBLRTM). If the difference between the two selected frequencies is small, it can be assumed that the cloud emissivtiy is independent of frequency. Using this approximation Equation 1 becomes independent of the cloud emissivity. The cloud height is then determined by selecting the cloud pressure that minimizes the difference between the right and left side of Equation 1.

In contrast to broadband sounders that have only a few channels in the CO_2 absorption region, hyperspectral measurements have thousands of channel pairs in this band. Overlap in hyperspectral channel weighting functions results in significant redundancy, which offers improvements in signal to noise when multiple channels pairs are averaged. In addition, the decrease in spectral width of the hyperspectral channels results in narrower weighting functions. These characteristics offer the opportunity to improve the accuracy of CO_2 Slicing (Smith, W. L. et al., 1990). However, the implementation of CO_2 Slicing to hyperspectral measurements has proven difficult as the large increase in the channel pairs introduces the added complexity of selecting optimal pairs. If opaque channel pairs are selected whose weighting function peak well above the cloud height the channels will have no cloud information and the CO_2 Slicing retrieval will have no skill. Channel pairs that peak near the cloud top altitude will maximize the cloud signal, resulting in the largest signal to noise ratio on the left side Equation 1.

In this investigation the hyperspectral CO_2 Slicing algorithm is implemented using a subset of channels in the CO_2 band. Each channel pair is applied to the CO_2 Slicing algorithm (Equation 1). If a unique cloud height is found, the cloud emissivity is computed using Equation 2.

Equation 2

$$N\varepsilon_{c,v}=\frac{I_v-I_{cl,v}}{I_{cld}-I_{cl,v}}$$

If the cloud emissivity is greater then 0.1 and less then 1.0 the channel pair solution is accepted. For the channel pairs found to converge to valid solutions a cost function is computed for all the valid channel pairs as described by

Equation 3

$$\Gamma_v=\sum_{v_{start}}^{v_{end}}\left(I_v-I_{cl,v}\right)-\varepsilon_v\left(I_{cl,v,p}-I_{cl,v}\right)$$

Where I_v is the measured S-HIS radiance in channel v, $I_{cl,v}$ is the calculated clear sky radiance, and $I_{cl,v,p}$ is the calculated opaque cloud radiances at pressure level p determined retrieved using CO_2 Slicing. V_{start} and V_{end} represent the channels used as pairs in the retrieval. The channel pair that minimizes Equation 3 is considered the optimal cloud height.

MLEV

Minimum Local Emissivity Variance (MLEV) is a cloud top retrieval algorithm designed to take advantage of hyperspectral measurements. MLEV uses the spectral channels between 750 – 950 cm $^{-1}$ that include CO_2 and water vapor absorption lines (Huang, H. L. et al., 2003). Hyperspectral measurements are capable of resolving the structure of these emission lines. In contrast, clouds have very little spectral structure across these wavelengths. The cloud emissivity is calculated using Equation 2 across and absorption line. The calculation of the cloud emissivity requires that the cloud altitude be known in order to calculate I_{cld} in the denominator of Equation 2. With an incorrect cloud height the spectral structure of the absorption line will not cancel in Equation 2 resulting in large spectral variability in the emissivity calculation. The cloud height that minimizes the spectral variability in Equation 2 yields the best estimate cloud height. The MLEV solving equations are illustrated in Equation 4 and Equation 5. Where I_v is the measured cloud radiance for channel v, $I_{cld,v}$ is the calculated opaque cloudy radiances, I_{cl} is the calculated clear sky radiance, N is the cloud fraction, and ε is the cloud emissivity. The cloud fractional emissivity is calculated for the channels between 750 –950 cm $^{-1}$ at each pressure level P_c. The pressure level that minimizes the spectral variation in this channel interval is considered the cloud pressure level. The implementation of MLEV requires calculations of the cloudy radiances at each pressure level available given in the temperature and moisture profile. For this analysis LBLRTM was used for these calculations.

Equation 4

$$LEV(P_c) = \sum_{v_1}^{v_2} (N\varepsilon_{c,v} - \overline{N\varepsilon_{c,v}})^2$$

Equation 5

$$\overline{N\varepsilon_{c,v}} = \frac{\sum_{v-(\Delta/2)}^{v+(\Delta/2)} (N\varepsilon_{c,v})}{\Delta v}$$

CO_2 Sorting

CO_2 Sorting is a new algorithm designed to overcome the complexity of choosing the optimal channel pairs needed in the CO_2 Slicing. Hyperspectral infrared measurements are capable of resolving the CO_2 band in great detail. A clear sky S-HIS measurement across the 15 μm CO_2 band (680 – 770 cm^{-1}) is shown in Figure 1. There is a trend to warmer brightness temperatures with increasing wave number due to the decrease in the opacity of the channels. However, the spectral structure of the CO_2 band results in significant fluctuation in the opacity of the channels. Assuming an atmosphere that decreases in temperature with height the measured brightness temperatures are proportional to the transparency of the channel. Using this relationship, if the channels are sorted relative to their clear-sky brightness temperatures they are also sorted relative to their opacity.

Sorted clear sky brightness temperatures are presented in Figure 1b. The Sorting results in a smoothly increasing function of brightness temperature starting with the coldest most opaque channel to the warmest transparent channels in the CO_2 band. The Sorting has ordered the channels by the atmospheric level at which the channel's weighting function is peaked.

The index of the channel order of the clear sky sorted spectrum can be applied to cloudy fields of view as presented in Figure 2a. The most opaque channel whose radiance includes significant cloud emission occurs where the clear and cloudy sorted spectrum deviate. This inflection point is illustrated in Figure 2a. The location of the inflection point is a function of the cloud altitude and cloud emissivity. For optically thick and high clouds the channels near the inflection point will have weighting functions that peak above the cloud altitude. In contrast, lower or optically thin clouds will have inflection points where the channel's weighting function peaks near the cloud altitude. This is illustrated in Figure 2b which presents the weighting functions of the channels selected by the inflection points in Figure 2a. The cloud height determined using the collocated CPL measurement is included in the figure.

In addition to the inflection point the slope of the sorted cloudy scene is related to the cloud emisivity. For optically thick clouds the slope of the cloudy spectrum will converge to the brightness temperature of the cloud. For optically thin clouds there is significant atmospheric emission from below the cloud. For these scenes the sorted spectrum will not converge to a constant brightness temperature because the emission detected by the transparent channels will include the emission from below the cloud.

It is possible to estimate the cloud height using the brightness temperature of the inflection point to interpolate the cloud height from an atmospheric temperature profile; however, the estimated cloud height derived from this method will be sensitive to the cloud emmisivity and is prone to over estimating the cloud height for optically thick and high clouds. To overcome this limitation a combined algorithm that uses CO_2 Sorting and CO_2 Slicing will be discussed.

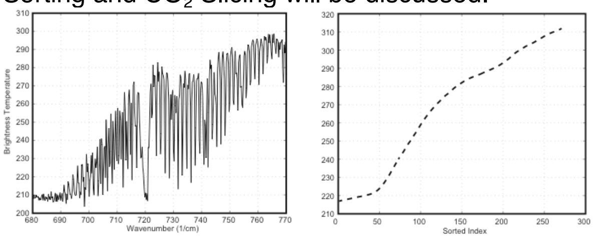

Figure 1 The S-HIS brightness temperature spectrum for the CO_2 absorption band is presented on the right figure. The right figure presents the brightness temperatures sorted from the coldest to warmest channels.

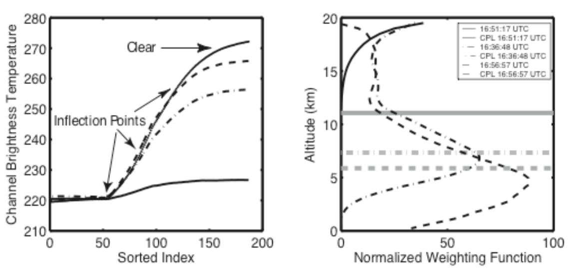

Figure 2 Cloudy sorted BT spectrums are presented with the clear sky sorted BT. The weighting functions of the channel picked to be the inflection point in the right figure are presented on the left.

The Hybrid CO_2 Slicing/Sorting Cloud Height Algorithm

The CO_2 Sorting algorithm offers a tool to overcome the difficulties of selecting optimal channel pairs as discussed in (CO_2 Slicing). The inflection point found by CO_2 Sorting represents the first channels with sensitivity to the cloud. Channels near this inflection point on the sorted spectrum will have weighting functions that peak near the cloud level maximizing the sensitivity of CO_2 Slicing. For clouds located in the middle and lower atmosphere the channel weighting function nearest the CO_2 Sorting inflection point peaks near the cloud altitude. For high clouds the weighting function of the channel nearest the CO_2 Sorting inflection point peaks well above the cloud (Figure 2). To compensate for this effect channels selected for CO_2 Slicing are offset towards warmer brightness temperatures on the sorted spectrum. The magnitude of the offset is linearly weighted so that inflection points found at cold brightness temperatures have a large offset while warmer inflection points (lower clouds) will have a minimal offset.

Collocation of imager and sounder data

The spatial distribution of clouds is highly variable. Quantitative comparisons of multiple instruments with varying fields of view and scan angles requires that the collocation of the instruments have errors less then the variability of the cloud structure in the field of view. For this research, a robust collocation algorithm originally developed for satellite collocation is adapted to work with the ER-2 instruments (Nagel, F. W., 1998). The collocation designates the instrument with the larger field of view as the master instrument. For this application the S-HIS is designated the master with its 100 mrad field of view. The collocation locates all fields of view of the secondary instrument or “Slave” instrument (S-HIS and CPL) that falls within each master filed of view.

For this application the instruments are located on the same platform (ER-2), simplifying the inverse navigation. The master footprint on the earth’s surface is difficult to describe mathematically (Nagel, F. W., 1998). The collocation uses a simplification described in Figure 3. The surface footprint of the master field of view is approximated as a “radar dish” centered on the surface of the earth. The collocation finds all slave geo-located fields of view whose angle α, measured between the slave geo-location and the center of the goe-located master field of view is less then the half angular width of the master instrument.

The geo-location for slave and master instruments is computed using the same geo-location algorithm to reduce errors caused by differences in geo-location algorithms used in the processed data for each instrument. For this reason, the collocation requires the aircraft position, role, heading, altitude, pitch, and instrument scan angle for both instruments. The instrument time is used to narrow the search region for finding collocated slave fields of view but is not used in the actual collocation. Because the collocation requires only the aircraft navigation information and master instrument field of view it is easily adaptable to multiple instruments. This adaptability allows for one algorithm to collocate both MAS and CPL with S-HIS.

While the collocation algorithm is robust, there are approximations and uncertainties. The largest source of errors is caused by the uncertainty of the relative pointing offset from nadir between the master and slave instruments. Each instrument is independently mounted on the ER-2. The angular offset from the aircraft nadir reference for each instrument is not known. It is estimated that errors as large as 3-4° from actual aircraft nadir may exist. Using an aircraft altitude of 20 km a 4° offset results in a 1.4 km error in the collocation, or about a field of view of the S-HIS.

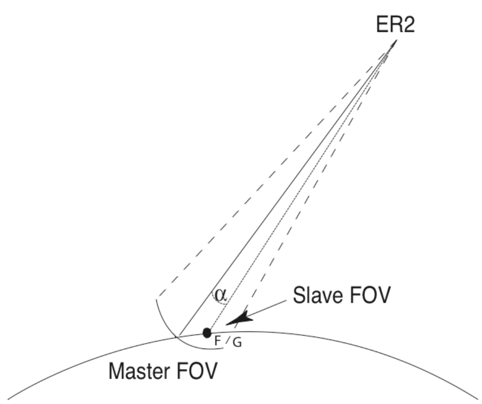

Figure 3 The collocation algorithm geometry is illustrated. The master field of view is defined as the half angular field of view of the master instrument (S-HIS). The angle between the slave instrument (MAS or S-HIS) geo-location (F) and the center axis of the master field is designated α in this figure. If α is less then the half angular field of view of the master instrument the slave pixel is considered to be within the field of view of the S-HIS.

Cloud Height Retrieval Validation

THORPEX Pacific

ER2 Flight Track 23:05 – 23:35 UTC

On February 22nd 2003 the ER2 flew over the Pacific Ocean west of Hawaii. During this flight high cirrus clouds with tops at 12 –13 km are detected by the CPL (Figure 4). Based on the CPL depolarization the cloud is comprised of ice with measured CPL cloud depolarization greater then 40%.

Figure 5 compares the CPL and the S-HIS cloud top retrievals. The CPL has maximum optical depth sensitivity of approximately 3.0. When interpreting the CPL cloud boundaries the actual cloud geometrical thickness may be larger then presented in Figure 5 if the total cloud optical depths are greater then 3.0. For this reason if the CPL does not detect a ground return below the cloud the CPL retrieved cloud base is not presented.

The beginning of the flight track is characterized by optically thin broken cirrus (Figure 5). For this time period (23:07 – 23:10) both the hybrid CO2Slicing/Sorting and the fixed channel pair CO2 Slicing algorithms detect the cloud but have difficulty detecting the height of the thin cirrus, with a large negative bias. Based on the CPL measurements the cirrus cloud progressively thickens after 23:11 UTC and by 23:16 UTC the CPL measured optical thickness is greater than 3.0. The S-HIS cloud top retrievals algorithms fail to detect the thin cirrus between 23:11- 23:12. The collocated CPL optical depth for this period was less than 1.0 but is gradually increasing. At approximately 23:12 both the CO_2 Slicing retrievals detects the cloud top however the algorithms underestimate the cloud height compared to the CPL. The agreement between the hybrid CO_2 Slicing/Sorting retrieval and the CPL cloud top height improves after 23:14 – 23:16 when the collocated CPL measured optical depth is greater then 2.0. In contrast, MLEV overestimates the cloud top by as much as 5.0 km when the CPL optical depths are1.0 –3.0. After 23:16 the CPL measured optical depths remain above 2.0 for the remainder of the flight track. As the cloud optical depths increase there is better agreement between the S-HIS cloud top retrievals and the CPL. The CO_2 Slicing fixed channel pair shows the greatest variability compared to MLEV and CO_2 Slicing/Sorting hybrid algorithm.

The distribution of the differences between the collocated CPL measured cloud top height compared to the S-HIS cloud top retrieval algorithms for individual S-HIS field of views is presented in Figure 5. The differences between the CPL and S-HIS are calculated using the mean cloud height of the CPL measurements found for each S-HIS field of view. If the S-HIS cloud top retrieval underestimates the cloud base relative to the CPL the difference will be negative while an overestimation results in a positive difference. Based on this distribution the hybrid CO_2 Sorting/Slicing retrieval is in close agreement with the CPL cloud top height for this flight track (Figure 5). The mean of the CO_2 Sorting/Slicing distribution for the entire flight track is –1.0 km with a standard deviation of 1.2 km. In comparison, the mean of both the CO_2 Slicing fixed channel pair and MLEV are similar with differences of –2.6 and –0.47 km respectively. Both MLEV and the CO_2 Slicing fixed channel pair algorithms have significantly more variability compared to the hybrid CO_2 Sorting/Sorting retrieval with standard deviations of 1.5 km for MLEV and 1.5 km for the fixed channel CO_2 Slicing retrieval. Based on these results the fixed channel pair CO_2 Slicing constantly under estimates the cloud top compared the hybrid CO_2 Slicing and MLEV algorithms.

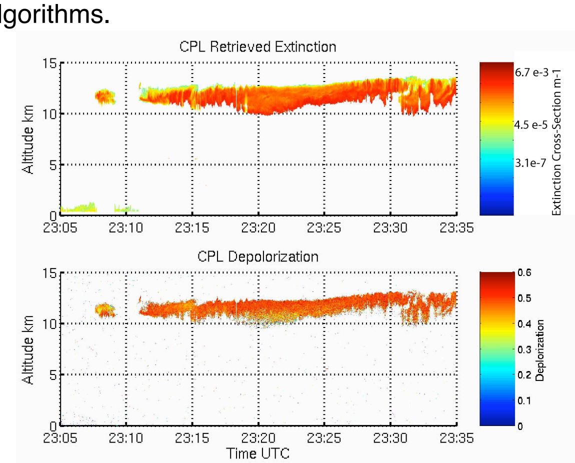

Figure 4 The CPL retrieved cloud extinction cross-section (m^{-1}) and depolarization obtained during the Pacific THORPeX experiment on February 22 2003.

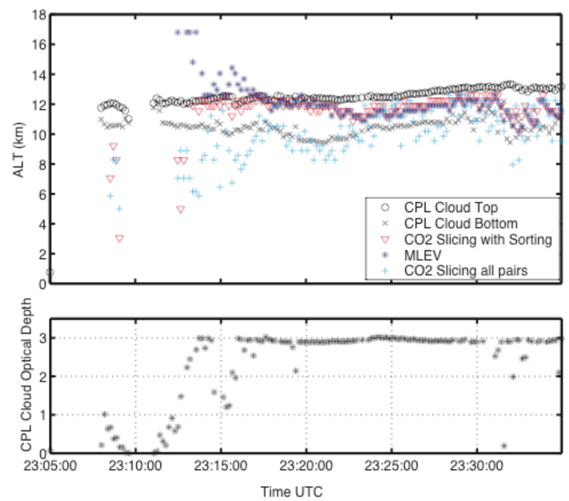

Figure 5 The S-HIS cloud top retrievals collocated with the CPL measured cloud top and base measurements from February 22nd 2003. The mean CPL measured optical depth is presented in the bottom figure. The cloud top, base and optical depth are the mean of all the CPL measurements found to be in each S-HIS field of view.

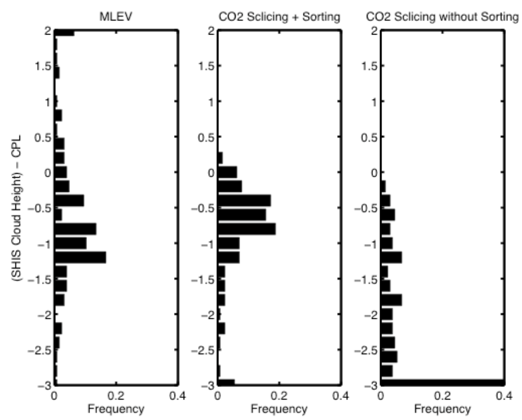

Figure 6 The frequency of occurrence of the differences between the S-HIS cloud top retrieval height compared to the mean of the collocated CPL cloud height is presented for the different S-HIS retrievals for the February 22nd 2003 flight.

ATReC Atlantic

The ER2 flew during the ATReC field experiment based in Bangor Mane in the fall of 2003 (REF). In addition to the MAS, CPL and S-HIS on the ER2 the NOAA G-4 and Citation flew during the experiment with an extensive array of insitu measurements. This investigation will focus on the December 5th 2003 the ER2 flight that over flew a variety of cloud types ranging from high cirrus to low stratus. Two different ER2 flight tracks are selected for their variety of cloud types.

ER2 flight track 16:30 – 1700 UTC

The ER2 flight segment is characterized by diverse cloud conditions. Between 16:30 – 17:15 the CPL measured cloud top and depolarization measurements indicate a rapidly changing cloud height and phase as presented in Figure 4. The CPL measured cloud depolarization varies between 2.0 - 50%. As previously discussed, depolarization less then 15% generally signify water clouds while depolarization greater then 25% are ice. The rapidly changing cloud conditions represent a challenging cloud top retrieval environment for the passive infrared.

The S-HIS cloud top retrievals collocated with the CPL and MAS retrieved cloud properties are presented in Figure 5. The S-HIS cloud fraction is retrieved by applying the collocated MAS pixels for each S-HIS field of view to the MAS cloud mask. The S-HIS cloud fraction is then computed by comparing the number of pixels found to be cloudy or probably cloudy to the total number of MAS pixels found for each S-HIS field of view.

The flight segment (16:30-16:33) has multiple cloud layers with geometric and optically thin mixed phased cloud at 7.0 km and water cloud at 4.0 km (Figure 4). The CPL retrieved optical depths for this period are between 0.5 –2.0. The CO_2 Slicing retrieval algorithms retrieve the 7.0 km cloud with varying skill as presented in Figure 5. The hybrid CO_2 Slicing/Sorting retrieval accurately detects the thin cirrus in a single S-HIS field. For this field of view the mean of the collocated CPL visible optical depths is approximately 1.0. The fixed channel pair CO_2 Slicing detects the thin cirrus in multiple fields of view but underestimates the cloud heights. MLEV fails to detect the cloud for this segment. Between 16:33 – 16:36 UTC only the fixed channel pair CO_2 Slicing retrieval detects the thin 5.0 km water cloud. After 16:36 UTC all the S-HIS cloud top retrievals detect the cloud. Both MLEV and the CO_2 Slicing/Sorting retrievals compare closely with the CPL. Compared to MLEV and the hybrid algorithms the CO_2 fixed channel pair retrieval has more variability (list ranges). This variability is illustrated by the distribution of the differences between the S-HIS cloud height retrievals and the collocated CPL cloud heights in Figure 6.

The peak of the hybrid CO_2 Slicing/Sorting difference distribution presented in Figure 6 compares closely with the CPL cloud heights with a mean of – 0.2 km and a standard deviation of 0.7. This is a significant improvement compared to the fixed channel CO_2 Slicing that has a larger offset and variance with a mean difference of –0.7 and standard deviation of 1.0 km. When interpreting Figure 6 the distributions for each algorithm is computed for only the fields of view that the algorithm detected the cloud. The larger differences found for the CO_2 fixed channel pair retrieval can be partially attributed to its increased sensitivity allowing detection of clouds with less accuracy but higher sensitivity. MLEV compares closely with the hybrid CO2Slicing/Sorting retrieval with a mean difference –0.38 km. 0.47 km.

The S-HIS cloud top retrievals demonstrates skill at detecting the cloud top altitude. However based on Figure 6 there can be large differences compared to the CPL For a small number of S-HIS fields of view there are differences of over –2.0 km during this flight segment. These large difference occurred when the S-HIS field of views had fractional cloud coverage based on the collocated MAS cloud mask.

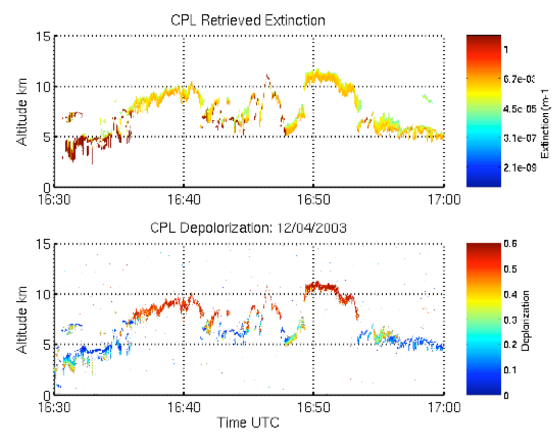

Figure 7 The CPL retrieved extinction and deploriazation from the Atlantic THORPeX experiment on December 5th 2003.

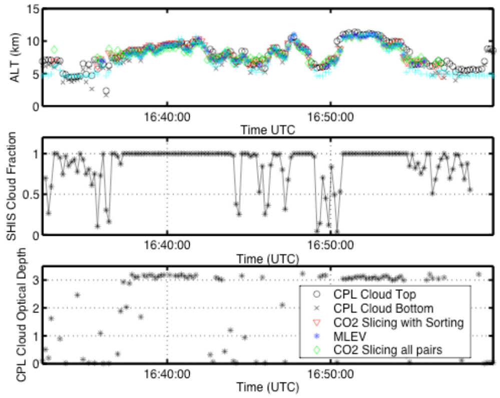

Figure 8 The S-HIS cloud top retrievals collocated with the CPL measured cloud top and base measurements from December 5th 2003. The cloud fraction is computed using the collocated MAS pixels for each S-HIS field of view. The MAS cloud mask is applied to the collocated MAS pixels and the cloud fraction is computed from the cloud mask results. The mean CPL measured optical depth is presented in the bottom figure. The cloud top, base and optical depth are the mean of all the CPL measurements found to be in each S-HIS field of view.

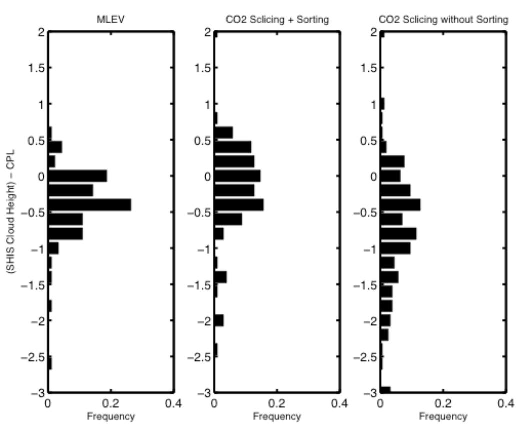

Figure 9 The frequency of occurrence of the differences between the S-HIS cloud top retrieval height compared to the mean of the collocated CPL cloud height is presented for the different S-HIS retrievals for the flight on December 5th 2003.

ER2 flight track 18:40 – 19:10 UTC

The ER2 over flew low stratus between 18:40 – 19:10 UTC (Figure 10). The collocated CPL cloud top altitudes vary between 500 meters to 3.0 km. Both MLEV and CO_2 Slicing hybrid failed to detect the low water clouds between 18:40 – 18:50 UTC. Surprisingly, the CO_2 Slicing fixed channel pair retrieval shows skill at detecting the low stratus. There are differences as large as 3.0 km compared to the CPL cloud top but for most fields of view the differences are less the a 1.0 km. The hybrid CO_2 Sorting/Slicing retrieval does not detect the 1.0 km stratus but does accurately detect 2.0 km water cloud at the end of the flight segment. MLEV fails to detect the low clouds for this segment.

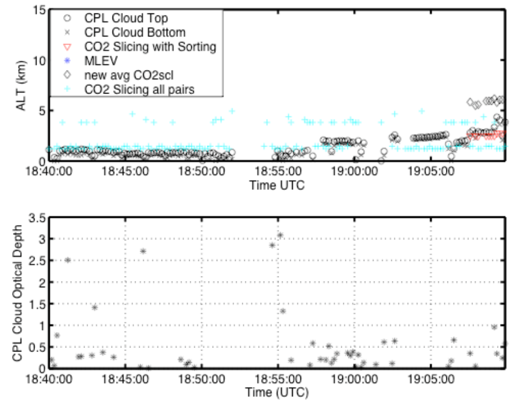

Figure 10 The S-HIS cloud top retrievals collocated with the CPL measured cloud top and base measurements from December 5th 2003. The mean CPL measured optical depth is presented in the bottom figure. The cloud top, base and optical depth are the mean of all the CPL measurements found to be in each S-HIS field of view. Only the CO_2 Slicing and CO_2 Slicing/Sorting algorithms are capable of detecting the low stratus clouds.

Discussion and Conclusion

To investigate the performance of hyperspectral cloud top retrieval algorithms a robust collocation of aircraft infrared hyperspectral (S-HIS), lidar (CPL) and high spatial resolution (MAS) measurements have been used. The collocated CPL measurements allow for quantitative analysis of the cloud top retrievals sensitivity to cloud height, optical depth, and cloud phase while the high spatial resolution of the MAS allows for the investigation of cloud fraction on the S-HIS cloud top retrievals.

As part of this investigation a new cloud top retrieval algorithm, CO_2 Sorting is presented. When combined with the fixed channel pair CO_2 Slicing the Sorting significantly improves the cloud top retrieval for high and mid-level clouds (4 –12 km) compared to the fixed channel pair CO_2 Slicing. An important finding from this investigation is that the cloud height and optical depth determines the optimal retrieval algorithm. Both MLEV and the hybrid CO_2 Slicing/Sorting retrieval demonstrate significant skill at detecting the cloud top altitude. However, the hybrid CO_2

Slicing/Sorting retrieval has the greatest sensitivity and the smallest altitude bias for optically thin and high clouds. The fixed channel pair CO_2 Slicing shows the greatest altitude bias and variance for mid and high level clouds. For low clouds (1.0 – 2.0 km) the CO2 fixed channel pair retrieval demonstrated surprising skill at detecting the low stratus. For this case MLEV failed to detect the low clouds and the hybrid CO2 Slicing/Sorting algorithm only detected the cloud when the cloud top, measured by the CPL, was above 2.5 km.

Future research plans include investigating additional collocated aircraft measurements and continued development of the CO2 Slicing/Sorting retrieval to improve the sensitivity of the algorithm to low clouds. Implementation of the CO2 Slicing/Sorting retrieval to satellite based hyperspecteral measurements (AIRS) are planed. This will include a thorough investigation of the satellite based cloud top retrieval performance using collocated satellite and aircraft measurements.

Huang, H. L., W. L. Smith, L. Li, P. Antonelli, X. Wu, R. O. Knuteson, B. Huang, and B. J. Osborne, 2003: Minimum local emissivity variance retrieval of cloud altitude and effective spectral emissivity simulation and initial verification. *Journal of Applied Meteorology*, **43,** 795-809.

King, M. D., W. P. Menzel, P. S. Grant, J. S. Myers, T. G. Arnold, S. E. Platnick, L. E. Gumley, S. Tsay, C. C. Moeller, M. Fitzgerald, K. S. Brown, and F. G. Osterwisch, 1996: Airborn Scanning Spectrometer for Remote Sensing of Cloud, Aerosol, Water Vapor, and Surface Properties. *Jounal of Atmopheric and Oceanic Technology*, **13,** 777-794.

McGill, M., D. Hlavka, W. Hart, V. S. Scott, J. D. Spinhirne, and B. Schmid, 2002: Cloud Physics Lidar: instrument description and initial measurement results. *Applied Optics*, **41,** 3725-3734.

Menzel, W. P., W. L. Smith, and T. R. Stewart, 1983: Improved Cloud Motion Wind Vector and Altitude Assignment Using Vas. *Journal of Climate and Applied Meteorology*, **22,** 377-384.

Nagel, F. W., 1998: The Association of Disparate Satellite Observations. *Second Symposium of Integrated Observing Systems*, Phoenix AZ, The American Meteorological Society.

Revercomb, H. E., V. P. Walden, J. Tobin, F. A. Anderson, N. C. Best, N. C. Ciganovich, T. G. Dedecker, T. Dirkx, S. C. Ellington, R. K. Garcia, R. Herbsleb, R. O. Knuteson, D. LaPorte, D. McRae, and M. Werner, 1998: Recent Results From Two New Aircraft-Based Fourier-Transform INterferometers: The Scannign High-resolution Interferometer Sounder adn the NPOESS Atmospheric Sounder Testbed Interferomter. *8th International Workshop on atmospheric Science from Space Using Foourier Transform Spectrometry*, Toulouse, France.

Smith, W. L., 1970: A regression method for obtaining real-time temperature and geopotential height profiles from satellite spectrometer measurements and its aplication to Nimbu-3 SIRS observations. *Monthy Weather Review*, **98,** 604-611.

Smith, W. L. and C. M. R. Platt, 1978: Comparison of Satellite-Deduced Cloud Heights with Indications from Radiosonde and Ground-Based Laser Measurements. *Journal of Applied Meteorology*, **17,** 1796-1802.

Smith, W. L. and R. Frey, 1990: On Cloud Altitude Determinations from High-Resolution Interferometer Sounder (His) Observations. *Journal of Applied Meteorology*, **29,** 658-662.